Author(s): Ruoho, Mikko & Juntunen, Taneli & Alasaarela, Tapani & Pudas, Marko & Tittonen, Ilkka

Title: Transparent, Flexible, and Passive Thermal Touch Panel

Year: 2016

Version: Pre print

Please cite the original version:

Ruoho, Mikko & Juntunen, Taneli & Alasaarela, Tapani & Pudas, Marko & Tittonen, Ilkka. 2016. Transparent, Flexible, and Passive Thermal Touch Panel. Advanced Materials Technologies. Volume 1, Issue 7. 2365-709X (printed). DOI: 10.1002/admt.201600204.

Transparent, Flexible and Passive Thermal Touch Panel

Mikko Ruoho, *Taneli Juntunen*, *Tapani Alasaarela*, *Marko Pudas*, and *Ilkka Tittonen**

M. Ruoho, T. Juntunen, Dr. T. Alasaarela, Prof. I. Tittonen

Department of Micro- and Nanosciences

Aalto University

FI-00076 Aalto, Finland

E-mail: ilkka.tittonen@aalto.fi

Dr. M. Pudas

Picosun Oy

Masalantie 365, FI-02430 Masala, Finland

This work presents a touch panel concept, which is enabled by a novel design of thin film thermocouples. The design offers a simple implementation by utilizing a single thin film to function as an array of thermocouples. The concept is demonstrated as a flexible, passive and highly transparent touch panel. The passive nature of the thermoelectric touch recognition allows the performance of the presented sensor to be optimal at moderate sheet resistance values of the transparent conductive layers. Hence, the concept is highly potential for low-cost large-area applications and does not rely on costly low sheet resistance materials such as indium tin oxide. The demonstrator presented in this work achieves a signal-to-noise ratio of 20 with a rise time of 90 ms and is able to distinguish individual touches, sweeping with finger, as well as touching by multiple fingers at the same time. In addition, the concept may also be used in other thermal distribution mapping applications.

Keywords: large-area, thermal, touch sensor, transparent, flexible electronics

I. INTRODUCTION

Touch sensor panels have become one of the key components in modern information devices. Currently, capacitive touch sensors are dominating within consumer electronics markets, and much of the research within display technologies is focused on the reduction of sheet resistance of the transparent conductors.[1–4] However, for large-area flexible applications, novel designs which take advantage of the trade-offs of the material properties are needed.[5] In addition, energy consumption of electrical devices, especially in mobile applications, has raised the interest towards low-power components. While thermoelectric materials are often proposed to improve the energy efficiency by the direct conversion of waste heat into electricity,[6] they may also be used to create passive or self-powered sensor systems in which thermal input may be utilized. Recent studies on the thermoelectric properties of transparent conductive materials[7–9] are giving rise to a novel field of transparent thermoelectrics allowing new applications within display technologies.

The commonly proposed concepts for touch detection are based on the capacitive, resistive, piezoelectric[10] and triboelectric effects.[11,12] Several of the current designs rely on the use of an array of multiple miniaturized sensing elements,[10,12–14] making large-area applications challenging. While the thermoelectric effect is commonly used to detect heat and also touch sensitivity has been proposed using arrays of individual thermocouples,[15–17] novel, more scalable designs allowing low-cost large-area touch sensors have gained little attention.

Here, we propose a thin film design allowing the use of a single film to function as an analogue of several in-plane thermocouples. Accordingly, the number of wiring can be halved in comparison to utilizing individual sensing elements. In addition, the thermoelectric signal generation has the advantage of being passive with sensing taking place electrically within a closed circuit. Accordingly, there are no strict limits for the sheet resistance of the active film nor for the leads used to probe the active film. Consequently, the concept does not rely on the low sheet resistance transparent conductor materials such as indium tin oxide (ITO) materials, and is highly applicable for large-area applications. The device is fabricated using a simple three-step process. The structure is transparent and flexible, requires no physical displacement of elements, and generates an electrical output signal on its own. In addition, the device utilizes a single sheet of low-cost active material requiring no patterning. While in this work we concentrate on human touch recognition, we note

that the operational principle is very general and can be used in many applications, ranging from human interface devices and biometry, to heat distribution mapping in industrial-scale processes and thermal characterization in research and development.

II. DESIGN AND WORKING PRINCIPLE OF THE ARRAY

The proposed structure consists of thin film thermocouples utilizing a single thermoelectric thin film as the active sensor material, which in this work was Al-doped ZnO. In addition, metallic contact pads are deposited on the thin film, and an insulating layer separates the thermoelectric thin film from metallic leads running between the edge of the sample and the contact pads. Each contact pad allows for probing of the Seebeck voltage at the point of contact between the pad and the thin film. The voltage is sensed with respect to a reference pad, which may be another contact pad or a dedicated contact at the periphery of the sample. In our design, we use a dedicated large-area contact at the edge of the sample, which is used as a common for all probe pads. The effective thermocouples are formed between the probe pads and the reference, and thus they are sensitive to the temperature differences between these points.

Figure 1 a) shows a schematic representation of the array, and photographs of the fabricated samples are shown in Figure 1 b) and c). The metallic leads are insulated from the underlying ZnO film and are used to read the voltage on the transparent ZnO film as can be seen in Figure 1. Otherwise the device is highly transparent.

III. MATERIALS AND METHODS

Three demostrator devices were fabricated with different properties. Atomic layer deposition was used to grow Al-doped ZnO on 100 μm thick PET (polyethylene terephthalate, Agfa-Gevaert NV), 600 μm thick glass and 50 μm thick polyimide (DuPont, Kapton CS) substrates using Picosun P-1000 ALD reactor. The deposition consisted initially of 100 ALD cycles of TMA and H_2O followed by roughly 600 ALD cycles of DEZn and H_2O. Samples 1 and 2 were doped with Al by introducing 4 ALD cycles of TMA and H_2O after every 200 cycles of DEZn and H_2O. Sample 3 contained a layered structure of an undoped ZnO layer, which was sandwiched between 2 highly doped layers. After initial 140 ALD cycles of TMA

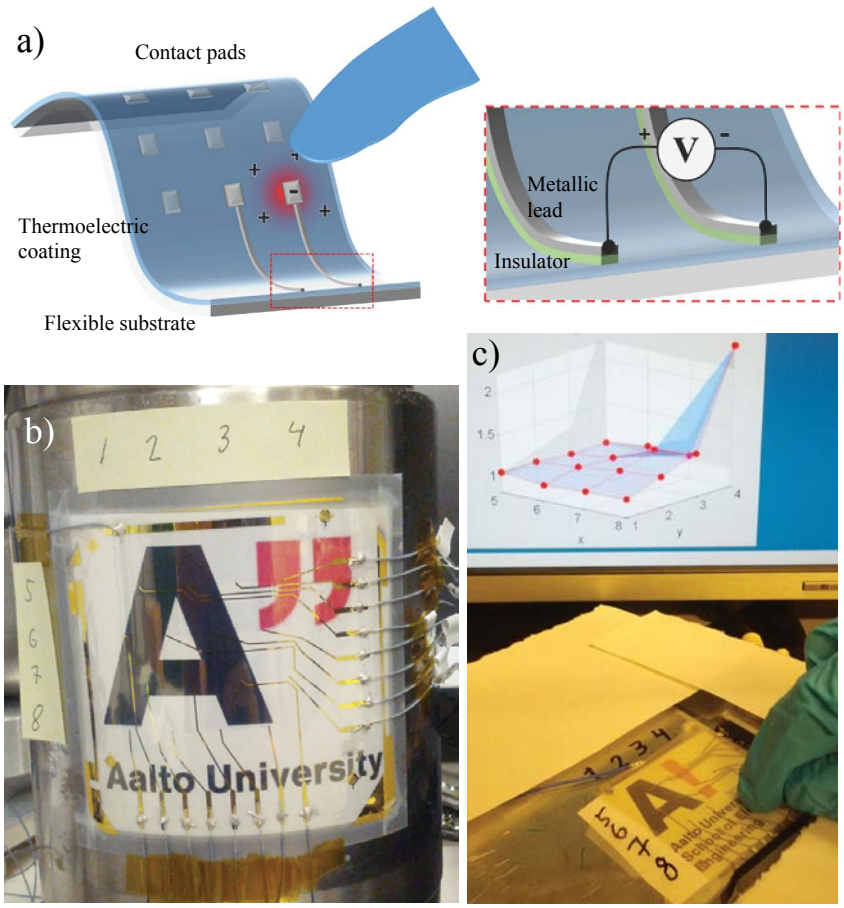

FIG. 1. Structure of the sensor element. a) Schematic representation of the sensor structure, and photographs of b) sensor of sample 3 bent to conform on a 100 mm diameter cylinder, and c) sensor of sample 1 and the voltage response when touching thermocouple at relative position coordinate of 4:8 with a finger wearing a nitrile glove. A program plots the relative change in the voltage as a function of location in real-time. The sensor rows and columns are labeled with 1 – 4 and 5 – 8, respectively.

and H_2O the pulsing sequence consisted of 7 supercycles consisting of 1 ALD cycle of TMA and H_2O and 30 ALD cycles of DEZn and H_2O, which was followed by 200 ALD cycles of DEZn and H_2O. The deposition was finished by 7 supercycles consisting of 1 ALD cycle of TMA and H_2O and 30 ALD cycles of DEZn and H_2O. Samples 1 and 2 were deposited in the same batch at the temperature of 150 °C and sample 3 at the temperature of 200 °C. The thicknesses of the films were measured by Plasmos SD 2300 ellipsometer from samples grown on silicon (100) in the same batch. The resulting thin film thicknesses were 131 nm for samples 1 and 2, and 117 nm for sample 3.

Fabrication of 4×4 sensing elements were carried out on a 50×50 mm^2 Al:ZnO film on substrate using electron-beam evaporation through stainless steel masks allowing simultaneous film deposition and patterning. At first, 60 nm of Al_2O_3 was deposited on the Al:ZnO coated substrates to insulate the leads and define the electrical contact pads. The contacting was done by depositing 20 nm of Ti and 160 nm of Au, and the same material was also used as leads running to the edge of the sample. Sample 1 was wired to the electronics by using a flexible PCB connector (TE Connectivity, 6-520315). For samples 2 and 3, wires were glued directly onto the sensor structure with conductive silver epoxy (CircuitWorks, CW2400).

Ti/Au contacts were fabricated on the thin films for van der Pauw and four point geometry. The samples were diced into 11 x 11 mm^2 pieces for the Hall- and 4 x 20 mm^2 pieces for the thermopower measurement. For Seebeck coefficient measurement, the samples on flexible substrates were cut and glued on a 4 x 20 mm^2 glass pieces using ceramic adhesive (PELCO, Product No. 16026).

Seebeck coefficients of the samples were determined using Linseis LSR-3 measurement system using a thin film adapter. Five different temperature gradients were used for the measurement carried out at an average temperature of 34 °C. The temperature differences and voltages obtained from the measurement system were linearly fitted and the Seebeck coefficient was obtained from the slope of the fit. Mobility and resistivity of the samples were obtained with Ecopia HMS-5300 measurement system using van der Pauw contact geometry.

Flexibility of the ZnO thin film was evaluated by collapsing radius tests. The outer bending radius was determined according to International Electrotechnical Commission standard draft 47/2199/NP. Keithley 2401 was used to evaluate the current-voltage characteristics of the film at each bend radius.

National Instruments 9213 data acquisition module was used to evaluate the voltage distribution of the sensor array, and it was visualized using a MATLAB software. High-speed voltage responses of the sensor array were also recorded with the data acquisition module.

IV. RESULTS AND DISCUSSION

The electrical and thermoelectric properties of the Al-doped ZnO films used as sensors were determined and the results are summarized in Table I. The thin film properties represent a relatively wide parameter space varying in resistivity from 3.1 to 7.3 mΩ cm and in Seebeck coefficient from -44 to -119 μV K^{-1}. In addition, the measured values for resistivity agree well with the values previously published for the material[9,18]. Furthermore, the Seebeck coefficient values are well in line with the obtained carrier concentration values.[19] Relatively wide material parameter range was utilized in order to determine the material parameters' influence on the functional performance of the sensors.

Figure 2 shows a typical transient response from the samples as a single thermosensor is touched by a gloved finger. We observe a sharp increase in the signal magnitude when the finger hits the sensor and the voltage quickly rises. The rise of the signal consists typically of two parts, as best seen in Figure 2 b). The transient signal first shows a fast linear rise of the signal roughly within the first 100 ms, after which the rise of the signal slows down eventually saturating at the peak value. Most of the responses show similar characteristics, although for samples 1 and 3 they are significantly faster. After the finger is removed we observe a gradual fall in the signal level as the heated thermocouple cools down.

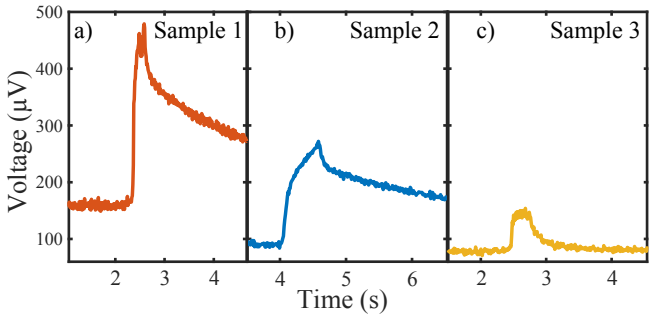

FIG. 2. Typical voltage response of all the samples as a function of time for a single thermosensor when pressed by a gloved finger.

Due to the relatively long time for the signal to return back to the original level, a more convenient means to recognize touches is done by monitoring the derivative of the signal as illustrated in **Figure 3** b) and SI Video 1, Supporting information. Figure 3 shows the resulting signal of four probe points touched one after another as well as the filtered derivative of the signal. The filtered derivative can be seen to be very effective in

determining the touches as well as minimizing the effect of the relatively long recovery time. As the recovery is slow and does not contain large transients, it is straightforward to filter. In addition, both the press and release of the finger induce a clear transient signal. The recovery time for the filtered signals is roughly 440 ms. Figure 3 a) also reveals that the electrical signal produced in the neighboring sensor does not noticeably hamper the output of the others, i.e., cross-talk between the channels is modest. In the SI Video 1, position sensitive touch detection is demonstrated by plotting the response when the transient in the signal of a thermocouple is above a predetermined threshold.

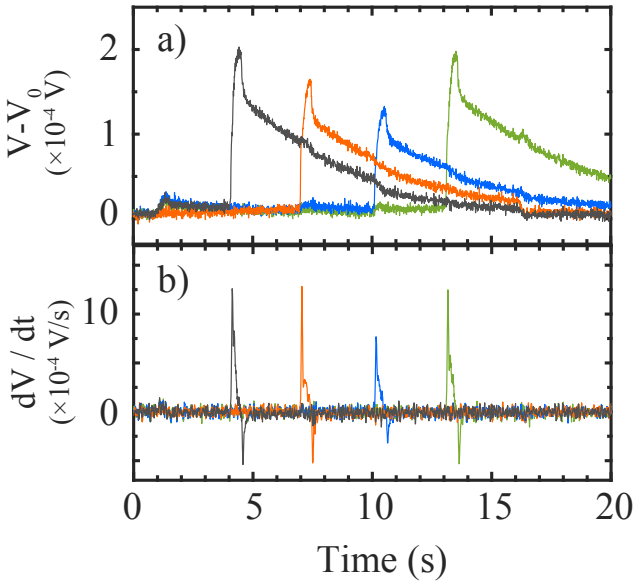

FIG. 3. Voltage responce of probes at 7:4, 8:1, 8:2 and 8:3 on Sample 2 when tapped lightly in three second intervals. Both the raw voltage data with the offset being removed a) and b) numerically filtered derivative of the signal is shown.

We demonstrate the output signal characteristics of the device under continuous and repetitive operation by recording the generated thermovoltage from a single lead when tapped every two seconds (**Figure 4** a), c), e)), and continuously pressed for five seconds in ten second intervals (Figure 4 b), d), f)). The responses shown in Figure 4 a), c) and e) were evaluated to assess the rise time and the signal-to-noise ratio (SNR = $\frac{P_{signal}}{P_{noise}}$) of a single sensing element. The average performance parameters are listed in Table II. The parameters were evaluated for both parts of the transient signal, the initial fast linear rise of

the signal and the whole peak-to-peak rise of the signal, while the peak-to-peak noise value was used to calculate both of the SNR values.

TABLE I. Properties of the substrates and deposited thin films at room temperature.

Name of sample	Substrate material	Substrate thickness (μm)	Thin film thickness (nm)	Resistivity (mΩ cm)	Carrier concentration ($\times 10^{19}$ cm^{-3})	Carrier mobility (cm^2/Vs)	Seebeck coefficient (μV/K)
Sample 1	PET	100	131	4.3	5.3	28	-73
Sample 2	Glass	600	131	7.3	3.1	28	-119
Sample 3	Kapton	50	117	3.1	13	13	-44

The results indicate that both samples 1 and 2 show the fast transient exhibiting a SNR of about 19. This fast phase for all the samples takes approximately 100 ms. The peak rise time for samples 1 and 3 is about 250 ms, whereas the signal of sample 2 does not have sufficient time to saturate and, consequently, the peak rise time indicated in Table II is equivalent to the duration of the press. The same can also be observed in Figures 4 c) and d). The peak SNR for samples 1 and 2 is relatively high at nearly 60, whereas the SNR values for sample 3 are rather modest, which is expected due to the low Seebeck coefficient.

The performance differences between the samples are explained by the Seebeck coefficient of the thin films as well as by the thermophysical properties of the substrate. In order to fully understand the role of the various material and geometrical parameters which affect the performance of the sensor, the responses were numerically analyzed using finite element method (**Figure 5** and Figures S1 – S5, supporting information).

The properties of the thin film play a role mainly in the magnitude of the signal via the Seebeck coefficient shown in Figure 5 a). Higher Seebeck coefficient translates directly into higher signal levels for the sensor. However, the resistivity, i.e., sheet resistance, of the thermoelectric thin film was found not to play a role in the signal shape or magnitude in the studied parameter range (Figure S3 (c), Supporting information). While this is partly explained by the absence of noise in the numerical analysis, it also highlights that the performance of the proposed touch detection scheme does not have a strict physical scaling law with respect to the thin film sheet resistance.

The chosen substrate has also a significant impact on the performance of the sensor.

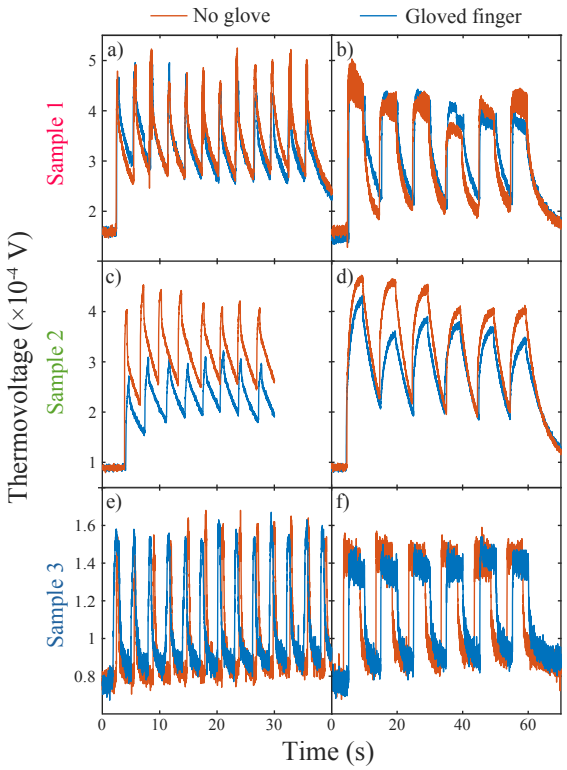

FIG. 4. Single-channel touch responses of the samples (sample 1 a) and b), sample 2 c) and b), sample 3 e) and f)) as pressed in two second intervals a), c) and e) as well as pressed for five seconds in ten second intervals b), d) and f). The signals are generated both with and without a nitrile glove.

By far, the largest influence stems from the substrate thickness, as thinner substrates lead to larger signal amplitudes. In addition, the speed of the transient, both in the rise and fall, is indirectly linked to the substrate thickness (Figure 5 b)). The effect can also be observed in Figure 4 f) as especially the fall times for sample 3 are shorter than those for the other samples. The effect can be easily understood, as objects with a smaller thermal mass heat up faster. Accordingly, having a thin substrate is beneficial in all aspects for the operation of the sensor. In addition, also the specific heat has a similar effect of increasing signal magnitude and shortening the fall time as illustrated in Figure 5 c). The general features of the device are thus akin to thermoelectric composites, wherein electrical features are dominated by thermoelectric material, while thermal properties are determined by the substrate.

The effects of the Seebeck coefficient and the substrate thickness explain the very similar

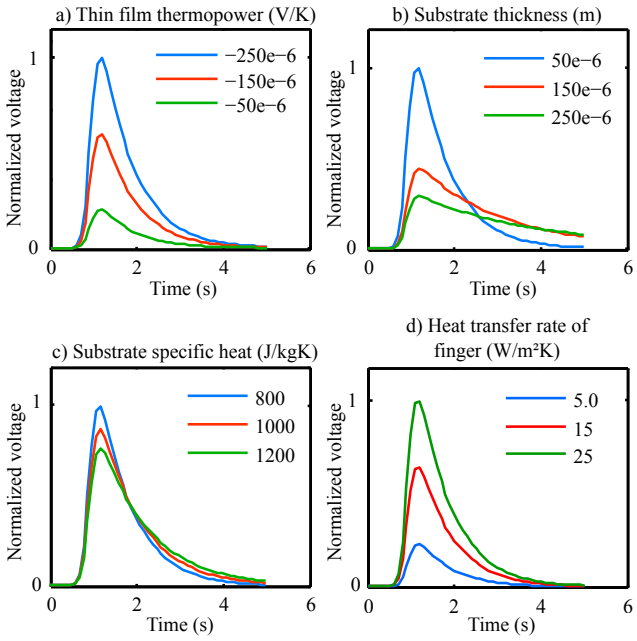

FIG. 5. Simulated touch responses with varying simulation parameters: a) Thin film thermopower, b) Substrate thickness c) Specific heat of the substrate and d) Heat transfer rate of finger.

TABLE II. Performance of the sensor array and key parameters of the thermoelectric thin film. The parameters that are called fast relate to the analysis of the first part of the transient response and conveys the average SNR obtained with the corresponding rise time, whereas the peak values address the maximum of the signal and the time it took to reach it. The pressing with a gloved finger was used for the evaluation.

Name of sample	Sheet resistance (Ω)	Seebeck coefficient (μV/K)	Power factor (μW/cmK^2)	Fast rise time (ms)	Peak rise time (ms)	Fast SNR (-)	Peak SNR (-)
Sample 1	324	-73	1.3	90	240	19.9	57.0
Sample 2	554	-119	1.9	110	500	19.2	59.2
Sample 3	262	-44	0.6	90	250	5.7	11.7

performance of samples 1 and 2 in terms of SNRs. The higher Seebeck coefficient of sample 2 was counteracted by the six times thicker glass substrate than that of the PET substrate. In addition, the sample 1 showed 50 % higher noise amplitude than sample 2, which also led to the very similar SNR values for both of the samples. The larger noise for sample 1 is likely related to the given method of wiring the sample to the electronics.

For samples 1 and 3, there is little difference whether they are touched with or without the nitrile glove. Accordingly, the difference between handling by gloved and bare finger seems to depend on the substrate material. While in general the larger heat transfer rate between the finger and the film leads to a larger signal (Figure 5 d)), the glove forms a thermal barrier between the finger and the sensor only when the substrate thermal conductivity is higher than that of the glove which is the case for sample 2. In addition, touching by a bare finger was noticed occasionally to lead to slightly increased noise, which is likely due to the electrical coupling of the finger and the sensor.

Additional test structures were fabricated and characterized in order to determine the spatial resolution (Figure S7, Supporting information) and to further demonstrate the scalability of the concept (Figure S8, Supporting information). The spatial resolution, as determined using the test structure, was shown to be less than 500 μm. The signal magnitudes were found to be independent of the length of the effective thermocouple with the scalability test sample illustrating the potential for large-area applications.

To illustrate the position-sensitive detection of a thermal contact point, i.e. touch, the voltage response of each of the leads was monitored in real-time. Figure 1 c) shows the relative voltage response of the sensor as a function of position. We observe a clear response as the voltage level is more than doubled when the sensor is touched. The device can distinguish between individual touches, sweeping with fingers, as well as touching by multiple fingers at the same time (see SI Video 2).

To demonstrate the use of the sensor on a non-planar surface, sample 3 was bent to conform a 100 mm diameter cylinder as shown in Figure 1 b). The device functionality is not altered by the procedure (SI Video 3). In order to test the response of the sensor to non-thermal input, the device was also manipulated by tweezers. The sensor was found to be insensitive to the touches by tweezers (SI Video 4) indicating that the observed signal is purely of thermal origin.

The flexibility of the Al:ZnO thin films used as the sensor material were evaluated, and the relative change in the resistance as the film is bent and released is depicted in **Figure 6**. Critical bending radii of roughly 4.5 mm for the sample 3 and 7 mm for the sample 1 are observed. The relatively low critical bending radius suggests that the flexibility provided by the ALD deposited thin film is highly compatible to, e.g., withstand roll-to-roll processing or conform to curved surfaces. The conformability of the fabricated sensor device is

demonstrated by bending sample 3 to conform a 100 mm cylinder (Figure 1 b)).

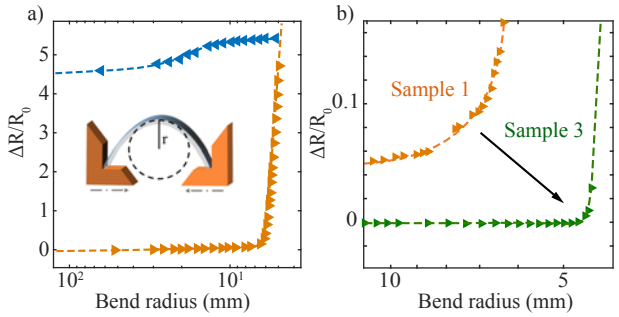

FIG. 6. Relative change of resistance as a function of bend radius for a) sample 1 and b) for sample 1 and sample 3. In a) orange right-pointing triangles represent the values while bending and blue left-pointing triangles represent the values while releasing the sample.

In a broader context, the operational principle of the touch screen may also be utilized in thermal distribution mapping applications. An example of this type of operation is illustrated is Figure S9 in the Supporting Information, where a thermal load is induced by a heated piece of silicon placed on the sensor. The thermal distribution created by the silicon piece can be clearly observed in the measured data.

V. CONCLUSIONS

In summary, we have presented a novel touch sensor design, which halves the required wiring by utilizing a single thin film to function as an array of thermocouples. In addition, we have demonstrated the performance to be independent of the sheet resistance of the material by passive thermoelectric touch detection. Moreover, the fabrication of the device can be carried out by relatively simple methods using a three-step process. As the demonstrator samples could be fabricated with materials that allow applications requiring flexibility and conformability, the concept is highly promising for low-cost large-area applications. To conclude, we wish to point out that the materials used in this work were chosen to be common and representative; however, a large range of different available materials and fabrication methods could also be used.

Supporting Information

Supporting Information is available from the Wiley Online Library or from the author.

Acknowledgements

We gratefully acknowledge the financial support from the Aalto ELEC Doctoral School and from the Academy of Finland project number 13140009. Part of the work has been performed in the TransFlexTeg, European Unions Horizon 2020 research and innovation program under grant agreement (No 645241) Large area transparent thin film thermoelectric devices for smart window and flexible applications http://www.transflexteg.eu/.

DuPont is acknowledged for providing experimental CS Series of Kapton. This research was partly performed at the Micronova Nanofabrication Centre, supported by Aalto University.

REFERENCES

[1]L. Zhang, Y. Zhou, L. Guo, W. Zhao, A. Barnes, H.-T. Zhang, C. Eaton, Y. Zheng, M. Brahlek, H. F. Haneef, et al., "Correlated metals as transparent conductors," Nature materials (2015).

[2]J.-Y. Lee, S. T. Connor, Y. Cui, and P. Peumans, "Solution-processed metal nanowire mesh transparent electrodes," Nano letters **8**, 689–692 (2008).

[3]K. S. Kim, Y. Zhao, H. Jang, S. Y. Lee, J. M. Kim, K. S. Kim, J.-H. Ahn, P. Kim, J.-Y. Choi, and B. H. Hong, "Large-scale pattern growth of graphene films for stretchable transparent electrodes," Nature **457**, 706–710 (2009).

[4]K. Tvingstedt and O. Inganäs, "Electrode grids for ITO free organic photovoltaic devices," Advanced Materials **19**, 2893–2897 (2007).

[5]A. Nathan, A. Ahnood, M. T. Cole, S. Lee, Y. Suzuki, P. Hiralal, F. Bonaccorso, T. Hasan, L. Garcia-Gancedo, A. Dyadyusha, S. Haque, P. Andrew, S. Hofmann, J. Moultrie, D. Chu, A. J. Flewitt, A. C. Ferrari, M. J. Kelly, J. Robertson, G. A. J. Amaratunga, and W. I. Milne, "Flexible Electronics: The Next Ubiquitous Platform," Proceedings of the IEEE **100**, 1486–1517 (2012).

[6]T. Kajikawa, *Thermoelectrics Handbook: Macro to Nano* (Taylor & Francis, Boca Raton, FL, 2010).

[7]Y. Inoue, M. Okamoto, T. Kawahara, Y. Okamoto, and J. Morimoto, "Thermoelectric properties of amorphous zinc oxide thin films fabricated by pulsed laser deposition," MATERIALS TRANSACTIONS **46**, 1470–1475 (2005).

[8]N. Vogel-Schäuble, Y. E. Romanyuk, S. Yoon, K. J. Saji, S. Populoh, S. Pokrant, M. H. Aguirre, and A. Weidenkaff, "Thermoelectric properties of nanostructured Al-substituted ZnO thin films," Thin Solid Films **520**, 6869 – 6875 (2012).
http://www.sciencedirect.com/science/article/pii/S0040609012008954

[9]M. Ruoho, V. Pale, M. Erdmanis, and I. Tittonen, "Influence of aluminium doping on thermoelectric performance of atomic layer deposited ZnO thin films," Applied Physics Letters **103**, 203 903 (2013).
http://scitation.aip.org/content/aip/journal/apl/103/20/10.1063/1.4831980

[10]D. Choi, K. Y. Lee, K. H. Lee, E. S. Kim, T. S. Kim, S. Y. Lee, S.-W. Kim, J.-Y. Choi, and J. M. Kim, "Piezoelectric touch-sensitive flexible hybrid energy harvesting nanoarchitectures," Nanotechnology **21**, 405 503 (2010).

[11]X. Wang, H. Zhang, L. Dong, X. Han, W. Du, J. Zhai, C. Pan, and Z. L. Wang, "Self-Powered High-Resolution and Pressure-Sensitive Triboelectric Sensor Matrix for Real-Time Tactile Mapping," Advanced Materials **28**, 2896–2903 (2016).

[12]B. Meng, W. Tang, Z.-h. Too, X. Zhang, M. Han, W. Liu, and H. Zhang, "A transparent single-friction-surface triboelectric generator and self-powered touch sensor," Energy Environ. Sci. **6**, 3235–3240 (2013).

[13]R. C. Webb, A. P. Bonifas, A. Behnaz, Y. Zhang, K. J. Yu, H. Cheng, M. Shi, Z. Bian, Z. Liu, Y.-S. Kim, et al., "Ultrathin conformal devices for precise and continuous thermal characterization of human skin," Nature materials **12**, 938–944 (2013).

[14]N. Sangeetha, M. Gauvin, N. Decorde, F. Delpech, P. Fazzini, B. Viallet, G. Viau, J. Grisolia, and L. Ressier, "A transparent flexible z-axis sensitive multi-touch panel based on colloidal ITO nanocrystals," Nanoscale **7**, 12 631–12 640 (2015).

[15]D.-H. Choi, J.-Y. Choi, E.-s. Kim, and J.-s. Rhyee, "Thermoelectric touch sensor," (2010), US Patent 8704112.

[16]C. Hou, H. Wang, Q. Zhang, Y. Li, and M. Zhu, "Highly Conductive, Flexible, and Compressible All-Graphene Passive Electronic Skin for Sensing Human Touch," Advanced Materials **26**, 5018–5024 (2014).

[17]F. Zhang, Y. Zang, D. Huang, C.-a. Di, and D. Zhu, "Flexible and self-powered

temperature-pressure dual-parameter sensors using microstructure-frame-supported organic thermoelectric materials," Nature communications **6** (2015).

[18]E. Yousfi, B. Weinberger, F. Donsanti, P. Cowache, and D. Lincot, "Atomic layer deposition of zinc oxide and indium sulfide layers for Cu(In,Ga)Se2 thin-film solar cells," Thin Solid Films **387**, 29 – 32 (2001), proceeedings of Symposium N on Thin Film Photovoltaic-materials of the E-MRS Spring Conference.
http://www.sciencedirect.com/science/article/pii/S0040609000018381

[19]D. L. Young, T. J. Coutts, V. I. Kaydanov, A. S. Gilmore, and W. P. Mulligan, "Direct measurement of density-of-states effective mass and scattering parameter in transparent conducting oxides using second-order transport phenomena," Journal of Vacuum Science & Technology A: Vacuum, Surfaces, and Films **18**, 2978–2985 (2000).
http://link.aip.org/link/?JVA/18/2978/1

LIST OF FIGURES